![Lund University seal]

LUND UNIVERSITY

Vibration measurements of a wooden building structure

Flodén, Ola

2016

Document Version:
Publisher's PDF, also known as Version of record

Link to publication

Citation for published version (APA):
Flodén, O. (2016). *Vibration measurements of a wooden building structure*. (TVSM-7000; No. TVSM-7162).
Division of Structural Mechanics, LTH.

Total number of authors:
1

LUND
UNIVERSITY

VIBRATION MEASUREMENTS OF A WOODEN BUILDING STRUCTURE

OLA FLODÉN

Structural
Mechanics

VIBRATION MEASUREMENTS OF A WOODEN BUILDING STRUCTURE

OLA FLODÉN

Contents

1 Introduction

The studies presented in this report were carried out at Lund University between July 2015 and October 2016. The studies are part of a project where numerical models for predicting low-frequency vibration transmission in wood buildings are developed. Vibration measurements were performed for a scaled-size wooden building structure representing part of a two-storey wood building. The measurements were performed for the complete structure and for sub-components at three different levels: structural components (viz. wood beams, particleboards and plasterboards), planar structures (viz. floor, ceiling and walls) and room structures. The results were evaluated at frequencies below 100 Hz; except for the results for the structural components, which were evaluated to obtain some higher-frequency modes as well. Material parameters of the structural components were determined through calibrating finite element (FE) models to measured data. The experimental results and optimised material parameters presented in this report will be used as input to model correlation studies regarding the low-frequency vibration transmission in wood buildings. These studies will be presented in a paper titled '*A multi-level model correlation approach for low-frequency vibration transmission in wood structures*'.

2 Experimental structure

The experimental structure, shown in Figure 2.1, represents a part of a two-storey timber volume element (TVE) building. TVE buildings are constructed by stacking pre-fabricated volume elements with elastomeric vibration isolators between storeys to reduce vibration transmission. The experimental structure consisted of two stacked rooms, where the upper room comprised a floor and four walls and the lower room comprised a ceiling and four walls. The two rooms were connected via 28 elastomer blocks placed between the walls of the two rooms, as shown in Figure 2.2. The planar structures consisted of wood frames with seven primary beams attached to edge beams placed perpendicular to their ends. The floor was covered by particleboards, whereas the ceiling and walls were covered by plasterboards. The walls were of two different types, which differed in the dimensions of the wood beams: apartment separating walls and facade walls. The two rooms contained two walls of each type. The apartment separating walls were placed along the edge beams of the floor and of the ceiling, whereas the facade walls were placed along the outermost primary beams.
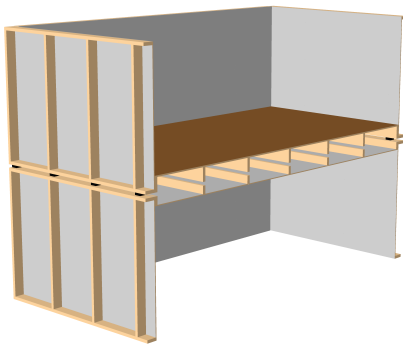
(a) Rendering of the structure when cut perpendicular to the primary beams in the floor and in the ceiling. Wood beams are shown in beige, particleboards in brown, plasterboards in grey and elastomer blocks in black.

(b) Photograph of the experimental setup used for the structure.

Figure 2.1: The experimental wooden building structure.
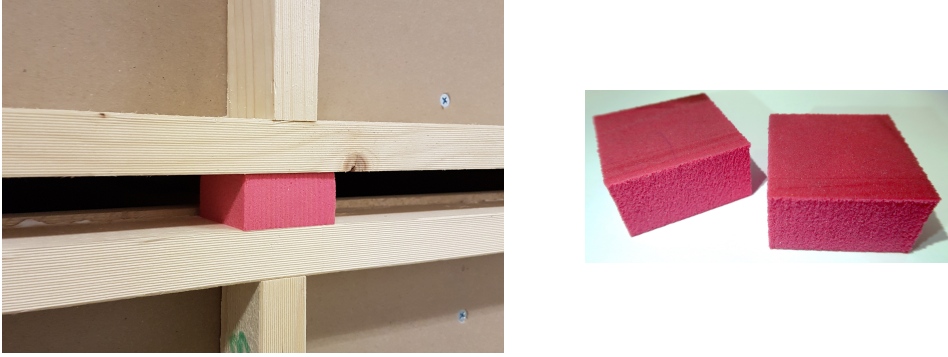
Figure 2.2: Photographs of the elastomer blocks placed between the walls of the two stacked rooms.

2.1 MATERIALS AND DIMENSIONS

The outer dimensions of the structure were 2600×2400×1900 mm^3. Table 2.1 presents the dimensions of the floor, ceiling and walls in terms of the cross-sectional dimensions of the beams ($h \times b$), the length and centre-to-centre distance of the primary beams (l and c/c, respectively), and the thickness of the boards (t). The elastomer blocks were 45×44×24 mm^3 in size and of the type Sylodyn NB [1]. The wood beams were made of spruce and of type G4-2 according to SS-EN 1611-1 [2]. The particleboards were of type P1 according to SS-EN 312 [3] and the plasterboards were of type A according to SS-EN 520 [4].

Table 2.1: Dimensions of the beams and boards in the floor, ceiling and walls. l and c/c are the length and centre-to-centre distance of the primary beams, h × b is the cross-sectional dimensions of the beams, and t is the thickness of the boards. Dimensions are in the unit of mm.

	l	c/c	h	b	t
Floor	2280	408	93	21	10
Ceiling	2280	272	54	21	6.5
Apartment separating walls	860	408	44	22	6.5
Facade walls	860	401	69	21	6.5

2.2 CONSTRUCTION

The wood frames in the floor, ceiling and walls were assembled by screwing the edge beams into the ends of the primary beams using 4 mm thick and 60 mm long wood screws. Figure 2.3 illustrates the connections between beams while Figure 2.4 shows the wood frame in the floor.
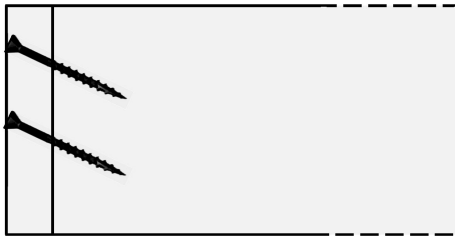
(a) Illustration.

(b) Photograph.

Figure 2.3: Connections between beams in the wood frames.

Figure 2.4: Photograph of the wood frame in the floor.
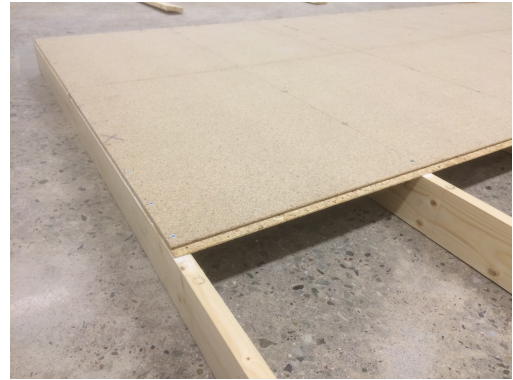
Figure 2.5: Photograph of the floor during mounting of the particleboards.

Figure 2.5 shows the floor during attachment of the particleboards, which were placed according to the drawing in Figure 2.6. The particleboards were glued to each other at their grooved-and-tongued edges and attached to the wood beams using both screws (4.2 mm thick and 42 mm long) and glue. The centre-to-centre distance between the screws was 100 mm along the outmost wood beams and 200 mm along the inner beams.

The plasterboards on the ceiling were placed according to the drawing in Figure 2.7, with a small gap between each of the boards. The walls were covered with one single plasterboard each. The plasterboards in the ceiling and walls were screwed to the wood frames using 3.5 mm thick and 25 mm long screws. The centre-to-centre between the screws was 70 mm at the edges of the plasterboards and 140 mm in their spans.

Figure 2.8 shows the upper room. It was assembled by first screwing the apartment separating walls into the sides of the edge beams of the floor. The facade walls were then screwed into
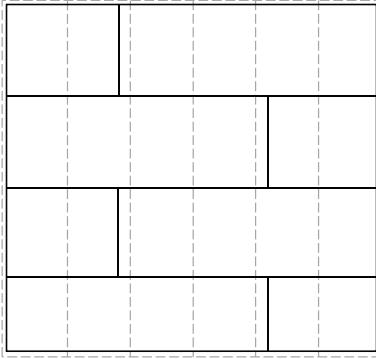
Figure 2.6: *Placement of particleboards on the wood beams in the floor. The dashed lines mark the wood beams.*
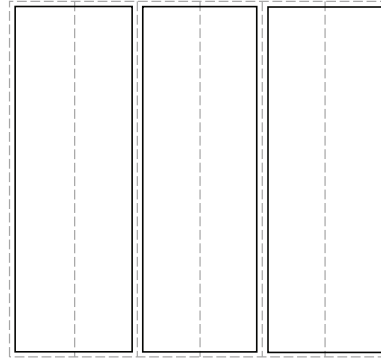
Figure 2.7: *Placement of plasterboards on the wood beams in the ceiling. The dashed lines mark the wood beams.*
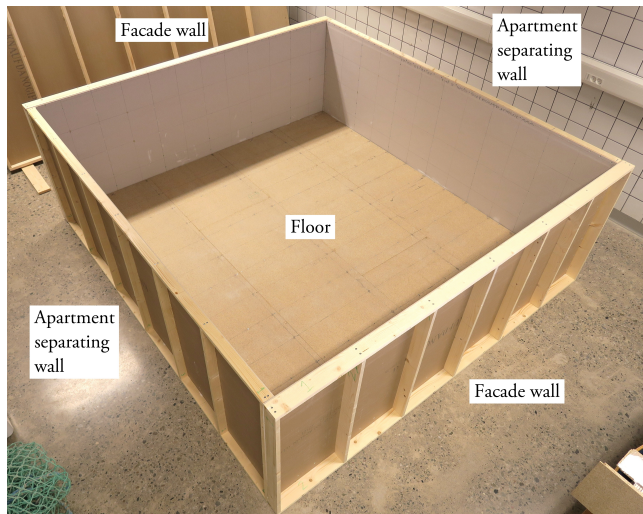
Figure 2.8: *Photograph of the upper room.*

the sides of the outermost primary beams of the floor and of the apartment separating walls. The walls were attached to the floor by screwing their edge beams into the outermost beams of the floor with 4.5 mm thick and 70 mm long screws placed at a centre-to-centre distance of 140 mm. Also, the plasterboards on the walls were screwed to the outermost beams of the floor with 3.5 mm thick and 25 mm long screws placed at a centre-to-centre distance of 140 mm along the beams. Figure 2.9 shows a junction between the floor and a wall, where the screws can be seen. The walls were connected to each other by screwing their outmost primary beams

Figure 2.9: *Photographs of a junction between the floor and a wall in the upper room. In the left photograph, the floor cannot be seen, but the arrow indicates its placement.*
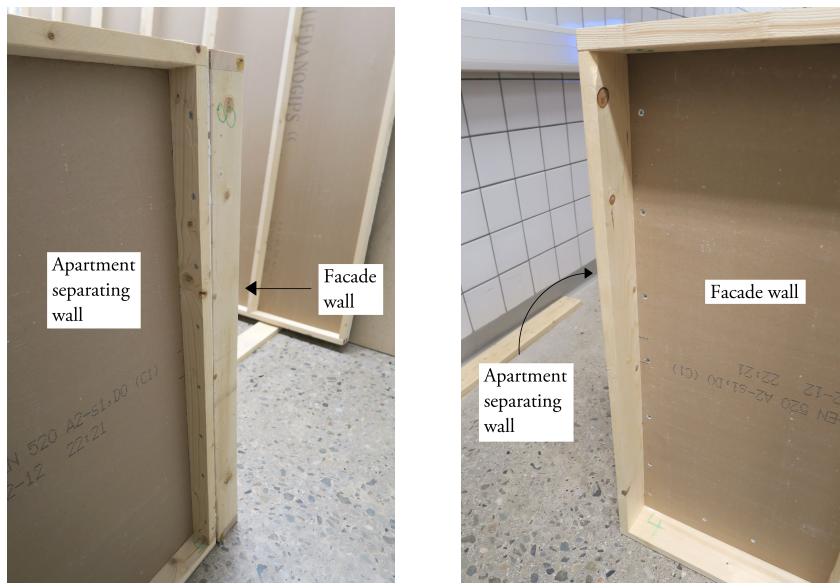
Figure 2.10: *Photographs of a junction between an apartment separating wall and a facade wall in the upper room. In the right photograph, the apartment separating wall cannot be seen, but the arrow indicates its placement.*

to each other with 4.5 mm thick and 70 mm long screws placed at a centre-to-centre distance of 100 mm. Also, the plasterboards on the facade walls were screwed to the beams of the apartment separating walls with 3.5 mm thick and 25 mm long screws placed at a centre-to-centre distance of 100 mm. Figure 2.10 shows a a junction between two walls, where the screws can be seen. The lower room was constructed in the same manner as the upper room. The elastomer blocks placed between the rooms were kept in place solely by frictional forces.

3 Measurements

Experimental modal analysis (EMA) was performed for the structural components, the planar structures and the two room structures. The vibration transmission in the complete structure was measured in terms of frequency response functions (FRFs). The measurements were carried out for frequencies below 100 Hz. Some higher-frequency modes of the structural components were also measured. The measurement results are presented in Appendix A.

3.1 LABORATORY CONDITIONS

All measurements were performed in a laboratory where the relative humidity was 50±5% and the temperature was 18±3° C during measurements as well as for 48 hours prior to measurements.

3.2 PROCEDURE

The measurements were performed in terms of impact testing, exciting the tested structures using hammers with integrated force sensors and measuring the resulting vibrations using accelerometers. The structures were suspended from the laboratory ceiling using elastic bands to mimic free boundary condition. The lowest eigenfrequencies of the structures were compared to the frequencies of the rigid body modes to ensure that they were well separated from each other. It was found that the rigid body modes, which had frequencies between 0–1.5 Hz, were significantly lower than the elastic modes; except for the first elastic mode of the floor and of the ceiling. It is pointed out in the results in Appendix A when a measured eigenfrequency is less than five times higher than the highest frequency of the rigid body modes.

The measurement procedure involved pre-test analyses of the tested structures to determine suitable excitation points and sensors positions. The pre-test were performed by studying simulated mode shapes, which were obtained through FE analyses of the structures. The FE models used for the pre-tests are described in Section 4.1. Uniform grids of excitation points were used. The resolution of these grids were decided by studying the simulated mode shapes to en-

sure that they could be distinguished from each other in the excitation points. The auto-MAC values, defined in Section 4.2, were used as objective measure of the similarity in mode shapes. If the off-diagonal terms in the auto-MAC matrix were below 0.2, the grid was adopted for the measurements.

Up to six accelerometers were used for each of the measured structures and these were placed in a fixed set of points. All six accelerometers were used for the EMA of the room structures, while five accelerometers were used for the floor and for the ceiling. Three accelerometers were used for the walls, while one accelerometer was used for the structural components. The measurement points were selected as a subset of the excitation points. This subset was determined by looping over all possible combinations of measurement points to find the combination that maximised an observability measure for the mode shapes. For one subset of excitation points, the observability measure was calculated by:

1. Normalising the simulated mode shapes by setting the maximum amplitude in each mode shape to unity.

2. Determining the maximum amplitude of each mode shape in the subset of excitation points.

3. Determining the smallest of the maximum amplitudes from the previous step. This value is the observability measure.

Signal processing and modal parameter estimation were performed using the Brüel & Kjær software PULSE Labshop/Reflex 19.0 [5]. The acceleration time signals were weighted with exponential windows and the force signals with cosine tapered windows. Through fast Fourier transforms (FFTs) of the measured force and acceleration signals, FRFs were estimated. The FFTs were calculated with a resolution of 0.25 Hz and an upper frequency limit depending on the frequency of the highest mode of interest. The estimated FRFs were averaged by repeating the measurements several times. Three repetitions were used for the structural components and for the planar structures, two repetitions were used for the room structures, and ten repetitions were used for the complete structure. The modal parameters were estimated by employing two methods implemented in PULSE Reflex 19.0 (the rational fraction polynomial method and a polyreference method in the time domain). The software's in-built modal selection algorithm was used. Manual corrections were made to remove possible duplicates in the mode sets while ensuring a good correlation between synthesised and measured FRFs. The mode sets were normalised to obtain real-valued vectors.

3.3 EQUIPMENT

The equipment used for the measurements is listed in Table 3.1.

Table 3.1: Measurement equipment used. All manufactured by Brüel & Kjær.

|	Type
Data aquisition frontends	LAN-XI 3050 A-060/A-042
Accelerometers, uni-axial	4507-001
Accelerometers, tri-axial	4524
Impact hammers	8206 & 8208

3.4 MEASUREMENTS OF STRUCTURAL COMPONENTS

3.4.1 Wood beams

EMA was performed for each wood beam in the experimental structure; a total of 90 beams. Six mode shapes and their eigenfrequencies were measured for each beam: the two first bending modes in each cross-sectional direction and the two first torsional modes. The measurement setup used for the beams is shown in Figure 3.1. A grid of 2×5 excitation points was employed. In one of the two rows of points, the beams were excited in the two cross-sectional directions. In the other row of excitation points, the beams were excited only perpendicular to the height direction. A tri-axial accelerometer was placed in one of the corners of the beams to measure the accelerations in the two cross-sectional directions. For the primary beams of the walls, only the first bending mode in each direction and the first torsional mode were measured. A grid of 2×3 excitation points was used for those beams. All tested specimens were weighed to be able to determine their densities. The measured eigenfrequencies and densities are presented in Appendix A.1.1. For some of the wood beams, all the eigenmodes that were intended to be measured were not captured; this is the reason to why some eigenfrequencies are missing in the results.

3.4.2 Particleboards and plasterboards

Measurements were performed for two specimens of each material. The measured particleboards and plasterboards were $750{\times}600{\times}10$ mm^3 and $760{\times}380{\times}6.5$ mm^3 in size, respectively. The first six eigenmodes of each specimen were measured. The measurement setup used for the particleboards and plasterboards is shown in Figure 3.2. A uniform grid of 3×5 excitation points was employed and the specimens were excited in the transversal direction. A uni-axial accelerometer was placed in one of the corners of the specimens. The tested specimens were weighed to be able to determine their densities. The measured eigenfrequencies and densities are presented in Appendix A.1.2.
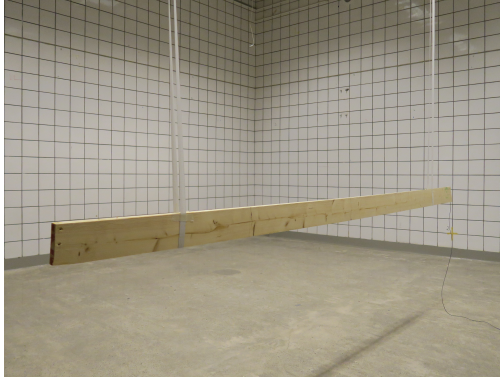
Figure 3.1: *Photograph of the measurement setup used for the wood beams.*
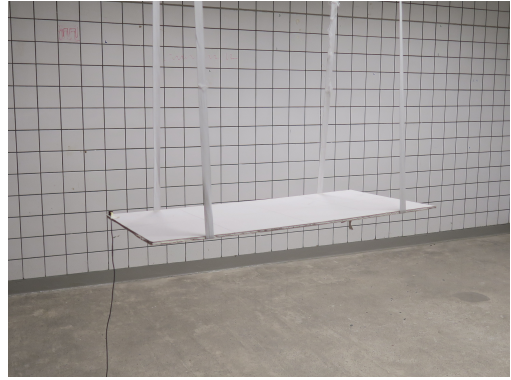
Figure 3.2: *Photograph of the measurement setup used for the particleboards and plasterboards.*

3.5 MEASUREMENTS OF PLANAR STRUCTURES

3.5.1 Floor

The measurement setup used for the floor is shown in Figure 3.3. The floor was excited in a total of 86 points. A uniform grid of 5×13 excitation points was used for the particleboard surface, which was impacted in the transversal direction. The seven primary beams were excited in three points each, perpendicular to their width direction. Five uni-axial accelerometers were used; three were placed on the particleboard surface and two on the beams. The measured eigenfrequencies and mode shapes are presented in Appendix A.2.1.

3.5.2 Ceiling

The measurement setup used for the ceiling is shown in Figure 3.4. The excitation points were chosen in the same way as for the floor, but with a grid of 9×13 points on the plasterboard surface. Hence, the ceiling was impacted in a total of 138 points. Five uni-axial accelerometers were used, all placed on the plasterboard surface. The measured eigenfrequencies and mode shapes are presented in Appendix A.2.2.

3.5.3 Walls

Measurements were performed for all eight walls in the structure: four apartment separating walls and four facade walls. The measurement setup used for the walls is shown in Figure 3.5. The same number of excitation points were used for all walls. The excitation points were placed on the plasterboard surface in a uniform grid of 5×13 points. Three uni-axial accelerometers
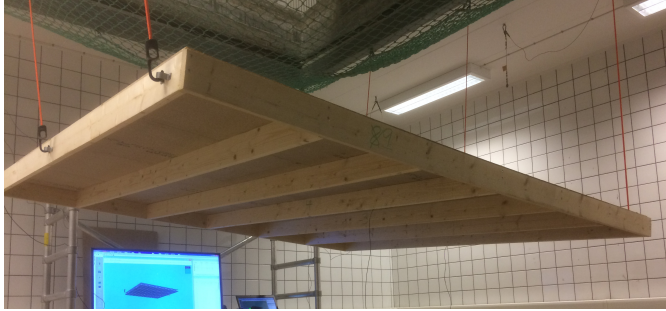
Figure 3.3: *Photograph of the measurement setup used for the floor.*

Figure 3.4: *Photograph of the measurement setup used for the ceiling.*

were used. The measured eigenfrequencies and mode shapes for the apartment separating walls are presented in Appendix A.2.3. The results for the facade walls are presented in Appendix A.2.4. In the results, the walls denoted '1' and '2' belong to the upper room, while those denoted '3' and '4' belong to the lower room.

3.6 MEASUREMENTS OF ROOM STRUCTURES

The measurement setup used for the two room structures is shown in Figure 3.6. All excitation points were placed on the particleboard and plasterboard surfaces. Uniform grids of excitation points were used for the surfaces of the floor, ceiling and walls. No points were placed at the connections between floor and walls and between ceiling and walls since the vibration amplitudes were expected to be low there. For the upper room, a grid of 5×11 excitation points was used for the floor surface, while grids of 4×11 points were used for the wall surfaces. Hence, a total of 231 excitation points were used for the upper room. For the lower room, a grid of 9×11 excitation points was used for the ceiling surface. Hence, a total of 295 points were used. For the measurements of each room structure, two accelerometers were placed on the floor/ceiling and one was placed on each wall. The measured eigenfrequencies, mode shapes and damping ratios are presented in Appendix A.3.1 for the upper room and in Appendix A.3.2 for the lower room. Only the results up to 50 Hz are presented because the measured mode shapes at higher frequencies had high complexity, i.e. they could not be approximated as real-valued.

Figure 3.5: Photographs of the measurement setup used for the walls.

3.7 MEASUREMENTS OF COMPLETE STRUCTURE

The measurement setup used for the complete structure is shown in Figure 2.1. The measurements were performed to determine FRFs for the vibration transmission from the floor in the upper room to the ceiling and walls in the lower room, and to determine driving point FRFs for the excitation points on the floor. The structure was excited in three points on the floor and the resulting accelerations were measured in four positions in the lower room; two on the ceiling, one on an apartment separating wall and one on a facade wall. Figure 3.7 shows the three excitation points (A–C) and the four measurement points (1–4). The measured FRFs are presented in Appendix A.4.

Figure 3.6: *Photograph of the measurement setup used for the room structures.*
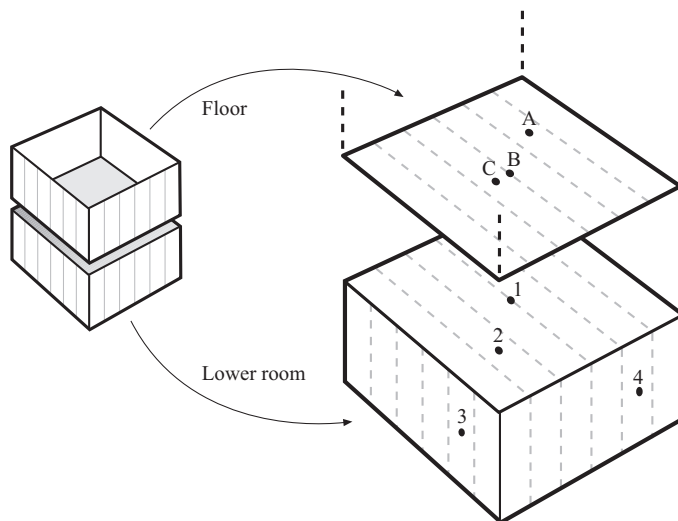
Figure 3.7: *Excitation points and measurement points employed for the measurements of FRFs in the experimental structure. The grey dashed lines indicate wood beams. The black dashed lines indicate the walls in the upper room.*

4 Determination of material parameters

Material parameters of the experimentally tested structural components (viz. wood beams, particleboards and plasterboards) were determined by calibrating FE models in order to fit the simulated eigenfrequencies to the measured ones.

4.1 FINITE ELEMENT MODELLING

FE models of the experimentally tested structural components were created. The modelling and analyses were performed using Abaqus/Standard 6.13 [6].

4.1.1 Material models

The materials were assumed to be linear elastic, homogeneous and orthotropic. Before performing the calibrations, initial material parameters had to be assigned to the FE models. Elastic parameters were collected from a wide range of publications to identify a feasible interval for each parameter. In some publications, the parameters are presented as normal distributions; the 95% confidence limits were taken from those publications. The initial parameters were chosen as the mid-points in the feasible intervals. However, the densities of the different materials were determined by weighing and measuring the dimensions of the structural components used in the experimental structure.

Parameters of spruce were collected from [7–10]. The intervals and the initial values used in the FE models of the measured wood beams are shown in Table 4.1. The parameters are given in terms of cylindrical coordinates (the longitudinal direction, L, the tangential direction, T, and the radial direction, R). E is the Young's modulus, G is the shear modulus, v is the Poisson's ratio and ρ is the density. The parameters in the radial and tangential directions were assumed to be equal, i.e. $E_T = E_R$, $G_{LT} = G_{LR}$ and $v_{LT} = v_{LR}$.

Table 4.1: *Material parameters of spruce in terms of the intervals identified from literature and the initial values used in the FE models. Stiffness parameters are in the unit of MPa and density in kg/m^3.*

	E_L	E_T, E_R	G_{LT}, G_{LR}	G_{RT}	ν_{LT}, ν_{LR}	ν_{TR}	ρ
Lower limit	5600	230	440	21	0.34	0.20	-
Upper limit	17000	1200	1600	125	0.72	0.60	-
Initial value	11000	700	1000	73	0.53	0.40	460

Parameters of particleboard were collected from [11–13]. In [11], the parameters are distinguished between the surface layers and the core layer of the boards. In [12, 13], however, the presented parameters are independent of the thickness direction. The intervals presented here are based on all types of values. In the FE model of the measured specimens, the parameters were assumed to be independent of the thickness direction. The intervals and the initial values used in the FE model are presented in Table 4.2. Directions 1 and 2 are the in-plane directions, while 3 is the out-of-plane direction. Direction 1 is the lengthwise direction of full-size particleboards, which is the widthwise direction of the measured specimens.

Table 4.2: *Material parameters of particleboard in terms of the intervals identified from literature and the initial values used in the FE model. Stiffness parameters are in the unit of MPa and density in kg/m^3.*

	E_1	E_2	E_3	G_{12}	G_{13}	G_{23}	ν_{12}	ν_{13}	ν_{23}	ρ
Lower limit	1300	1200	200	570	170	150	-0.06	0.23	0.20	-
Upper limit	5500	4800	570	1800	400	370	0.44	1.32	1.27	-
Initial value	3400	3000	390	1200	290	260	0.19	0.78	0.74	750

Parameters of plasterboard were collected from two manufacturers [14, 15] and two research papers [16, 17]. Only the Young's moduli are presented in the references: [14–16] present orthotropic parameters for the in-plane directions of the boards, while [17] presents isotropic parameters. The intervals for the remaining parameters were chosen without any a priori knowledge. The out-of-plane Young's modulus, E_3, is likely to be lower than the in-plane moduli, E_1 and E_2, because of the paper-coating of the boards, which contributes to the bending stiffness. The lower limit was therefore set to 10% of the limit for the in-plane parameters. The interval for E_3 was used also for the three shear moduli. The intervals and the initial values used in the FE model are presented in Table 4.3. Direction 1 is the lengthwise direction of full-size particleboards, which is the widthwise direction of the measured specimens.

Table 4.3: *Material parameters of plasterboard in terms of the intervals identified from literature and the initial values used in the FE model. Stiffness parameters are in the unit of MPa and density in kg/m^3.*

	E_1	E_2	E_3	G_{12}	G_{13}	G_{23}	ν_{12}	ν_{13}	ν_{23}	ρ
Lower limit	1600	1600	150	150	150	150	0.0	0.0	0.0	-
Upper limit	2500	2000	2500	2500	2500	2500	0.5	0.5	0.5	-
Initial value	2000	1800	1000	1000	1000	1000	0.25	0.25	0.25	760

4.1.2 Discretisations

The models were meshed with 20-node solid hexahedral elements with quadratic interpolation and reduced integration. Mesh convergence was performed for the FE models by ensuring that the errors in the simulated eigenfrequencies (belonging to the measured eigenmodes) were less than 0.1% when compared to densely meshed models. As an example, the mesh convergence studies resulted in the primary beams of the floor being meshed with 2×4×21 elements.

4.1.3 Models for pre-analyses

The models of the structural components were assembled to create FE models of the planar structures and of the room structures. These were used for pre-test analyses for the measurements of those structures. The joints in the assembled structures were modelled as fully coupled. The joints between beams and boards were implemented by using one single mesh for each planar structure, so that the beams and boards shared mesh nodes. The joints between planar structures were implemented by using Lagrange multipliers. The plasterboards in the ceiling were modelled as a single continuous board. The same was done for the particleboards in the floor.

4.2 ERROR METRICS

The calibration procedure presented in Section 4.3 is based on comparisons between results from simulations and measurements. The error metrics used for the comparisons are defined in this section.

Normalised relative frequency difference

To compare the eigenfrequencies obtained from simulations to those from measurements, the normalised relative frequency difference (NRFD) was employed, defined as

$$\text{NRFD} = \frac{f_i^{sim} - f_j^{exp}}{f_j^{exp}}, \tag{4.1}$$

where f_i^{sim} is the ith eigenfrequency from simulations and f_j^{exp} is the jth eigenfrequency from measurements.

Modal assurance criterion

The NRFD value is relevant only if the simulated and measured eigenfrequencies belong to corresponding mode shapes. The MAC value was employed to quantify the similarity in mode shapes. It is defined as

$$\text{MAC} = \frac{\left|(\Phi_i^{sim})^T(\Phi_j^{exp})\right|^2}{(\Phi_i^{sim})^T(\Phi_i^{sim})(\Phi_j^{exp})^T(\Phi_j^{exp})}, \tag{4.2}$$

where Φ_i^{sim} is the ith simulated mode shape and Φ_j^{exp} is the jth measured mode shape. The MAC value falls between 0 and 1, where 1 implies perfect correlation between the two mode shapes.

Two mode sets can be compared to each other by calculating the MAC values according to Equation (4.2) for all possible combinations of modes. This results in a matrix of MAC values that is referred to as the cross-MAC matrix. Comparing a mode set to itself is referred to as auto-MAC. The diagonal terms in an auto-MAC matrix are by definition equal to one. The off-diagonal terms, however, can be used to measure the similarity between mode shapes within the same set.

4.3 CALIBRATION PROCEDURE

The material parameters in the FE models of the structural components were optimised by fitting the simulated eigenfrequencies to the measured eigenfrequencies for each specimen. It was ensured that the NRFD values were based on well-correlated mode shapes between simulations and measurements. For the particleboards and plasterboards, the MAC values were higher than 0.9. For the wood beams, the MAC values were higher than 0.7 and about 0.9 in average. The calibrations of the FE models did not have any appreciable effect on the MAC values. The objective function used in the optimisations was the sum of squared NRFD

values:

$$g\left(\mathbf{x}\right) = \sum_{i=1}^{n} \left(\frac{\left| f_i^{sim}\left(\mathbf{x}\right) - f_i^{meas} \right|}{f_i^{meas}} \right)^2, \tag{4.3}$$

where $\mathbf{x}$ contains the material parameters that were optimised and n is the number of eigen-frequencies included in the optimisations. The NRFD values are squared in the objective function to make it smoother and suitable for optimisations. The elastic parameters discussed in Section 4.1.1 were optimised for each tested specimen of the structural components. The optimisations were performed in three steps:

1. **Sensitivity analysis.** The parameters were varied one at a time within the interval limits presented in Section 4.1.1, and the effects on the simulated eigenfrequencies were studied. Only the parameters with appreciable effect on the NRFD values were optimised in steps 2 and 3. For the remaining parameters, the initial values were used.

2. **Grid search.** The intervals for the material parameters presented in Section 4.1.1 were divided into ten steps each and the objective function was evaluated for all combinations of parameter values. The results provided an estimate of the optimal parameters.

3. **Newton optimisation.** The parameters from step 2 were used as initial values for a multi-dimensional Newton optimisation. Iterations were performed until each of the parameters were updated with a maximum of 0.1% of its value.

4.4 RESULTS

The NRFD values obtained using the calibrated models were below 4% for each measured eigenfrequency and about 1% in average. The sensitivity analyses for the wood beams unveiled that two parameters have appreciable effect on the eigenfrequencies of the wood beams, E_L and $G_{LR} = G_{LT}$. The remaining parameters affect the NRFD values with less than 0.5%. For several of the primary beams in the facade walls, the torsional modes were not captured in the measurements. As a consequence, $G_{LR} = G_{LT}$ could not be calibrated for those beams. To determine those parameters, a linear regression between E_L and $G_{LR} = G_{LT}$ was established based on the optimised values for all other beams in the experimental structure. The regression model was employed to determine $G_{LR} = G_{LT}$ for the primary beams of the facade walls by using the optimised values of E_L as input. The optimised material parameters of all 90 wood beams in the experimental structure are presented in Appendix B.1. Normal distributions of the optimised parameters are also presented.

For the particleboards and plasterboards, three parameters were found to have an appreciable effect on the eigenfrequencies: E_1, E_2 and G_{12}. The remaining parameters affect the NRFD values with less than 1%; except for ν_{12}, which affect the NRFD values with up to 8%. This is, however, low compared to E_1, E_2 and G_{12}, which affect the NRFD values with up to 130%. The optimised material parameters of the measured specimens are presented in Appendix B.2.

References

[1] Getzner Werkstoffe GmbH (2008), *Sylodyn NB, product data sheet*, 2016-10-25: https://www.getzner.com/en/products/sylodyn.

[2] Swedish Standards Institute (2000), *SS-EN 1611-1: Sawn timber – Appearance grading of softwoods – Part 1: European spruces, firs, pines and Douglas firs*, SIS, Stockholm, Sweden.

[3] Swedish Standards Institute (2010), *SS-EN 312: Particleboards – Specifications*, SIS, Stockholm, Sweden.

[4] Swedish Standards Institute (2009), *SS-EN 520: Gypsum plasterboards – Definitions, requirements and test methods*, SIS, Stockholm, Sweden.

[5] Brüel & Kjær (2014), *PULSE Reflex 19.0*, Brüel & Kjær Sound & Vibration Measurement A/S, Nærum, Denmark.

[6] Dassault Systèmes (2013), *Abaqus 6.13 manual*, Dassault Systèmes Simulia Corp., Providence, United States.

[7] Larsson, D., Ohlsson, S., Perstorper, M., Brundin, J. (1998), *Mechanical properties of sawn timber from Norway spruce*, Holz als Roh- und Werkstoff **56**, 331–338.

[8] Berbom Dahl, K. (2009), *Mechanical properties of clear wood from Norway spruce*, Ph.D. thesis, Norwegian University of Science and Technology, Trondheim.

[9] Kretschmann, D. (2010), *Wood handbook – Wood as an engineering material: Chapter 5 – Mechanical properties of wood*, US Dept of Agriculture, Forest Service, Forest Products Laboratory.

[10] Danielsson, H. (2013), *Perpendicular to grain fracture analysis of wooden structural elements – Models and application*, Ph.D. thesis, Lund University, Sweden.

[11] Wilczyński, A., Kociszewski, M. (2011), *Determination of elastic constants of particleboard layers by compressing glued layer specimens*, Wood Research **56(1)**, 77–92.

[12] Najafi, S.K., Bucur, V., Ebrahimi, G. (2005), *Elastic constants of particleboard with ultrasonic technique*, Materials Letters **59**, 2039–2042.

[13] Nemli, G., Aydin, I., Zekovic, E. (2007), *Evaluation of the properties of particleboard as function of manufacturing parameters*, Materials & Design **28**, 1169–1176.

[14] Knauf Danogips (2016), *Classic Board, product data sheet*, 2016-10-11: http://byggsystem.knaufdanogips.se/index.php/filbibliotek/produktdatablad/details/24/2/produktdatablad-classic-board.

[15] Gyproc Saint-Gobain (2016), *GNE Normal, product data sheet*, 2016-10-11: http://gyproc.se/node/2057.

[16] Cramer, S.M., Friday, O.M., White, R.H., Sriprutkiat, G. (2003), *Mechanical properties of gypsum board at elevated temperatures*, in: *Proceedings of Fire and Materials 2003*, San Fransicso, US.

[17] Rahmanian, I. (2011), *Thermal and mechanical properties of gypsum boards and their influence on fire resistance of gypsum board based systems*, Ph.D. thesis, University of Manchester, UK.

Appendices

A Measurement results

A.1 STRUCTURAL COMPONENTS

A.1.1 Wood beams

Table A.1: *Measured densities (kg/m³) and eigenfrequencies (Hz) for the wood beams of the floor. Beams 1–7 are primary beams and beams 8–9 are edge beams.*

Specimen	Density	Bending, width		Bending, height		Torsion	
		First	Second	First	Second	First	Second
1	444	21.4	59.3	91.5	243	–	236
2	509	21.8	59.3	96.9	253	113	229
3	522	22.1	61.6	95.2	251	109	216
4	421	20.3	55.9	86.8	229	101	202
5	503	22.4	60.8	99.2	257	109	221
6	437	20.8	58.7	89.8	242	–	223
7	450	20.8	56.6	91.1	240	107	217
8	468	16.8	47.4	74.2	201	103	206
9	500	17.4	48.3	75.8	205	106	210

(Eigenfrequencies header spans Bending, width / Bending, height / Torsion columns)

Table A.2: *Measured densities (kg/m^3) and eigenfrequencies (Hz) for the wood beams of the ceiling. Beams 1–7 are primary beams and beams 8–9 are edge beams.*

| | | Eigenfrequencies | | | | | |
| | | Bending, width | | Bending, height | | Torsion | |
Specimen	Density	First	Second	First	Second	First	Second
1	426	22.4	61.3	57.8	154	169	337
2	462	20.4	56.9	50.7	141	173	349
3	441	23.3	64.5	58.9	160	167	330
4	521	22.1	61.3	54.8	148	169	339
5	432	22.4	61.5	55.8	150	170	335
6	464	20.7	57.9	50.9	142	180	356
7	488	24.2	66.8	62.1	166	165	331
8	510	18.2	49.9	47.4	129	179	354
9	424	17.1	49.6	45.6	125	158	314

Table A.3: *Measured densities (kg/m^3) and eigenfrequencies (Hz) for the wood beams of apartment separating wall 1. Beams 1–7 are primary beams and beams 8–9 are edge beams.*

| | | Eigenfrequencies | | | | | |
| | | Bending, width | | Bending, height | | Torsion | |
Specimen	Density	First	Second	First	Second	First	Second
1	474	136	–	270	–	544	–
2	420	117	–	242	–	528	–
3	483	143	–	279	–	568	–
4	473	138	–	279	–	559	–
5	406	142	–	276	–	532	–
6	482	142	–	281	–	553	–
7	464	139	–	274	–	573	–
8	454	19.4	52.1	38.0	–	196	400
9	416	19.3	53.7	38.5	108	181	–

Table A.4: Measured densities (kg/m^3) and eigenfrequencies (Hz) for the wood beams of apartment separating wall 2. Beams 1–7 are primary beams and beams 8–9 are edge beams.

Specimen	Density	Eigenfrequencies					
		Bending, width		Bending, height		Torsion	
		First	Second	First	Second	First	Second
1	371	123	–	244	–	512	–
2	529	153	–	278	–	582	–
3	455	146	–	284	–	549	–
4	368	134	–	265	–	499	–
5	410	135	–	267	–	534	–
6	472	133	–	271	–	559	–
7	415	138	–	270	–	550	–
8	459	17.7	50.3	35.6	101	200	396
9	492	19.4	51.6	38.0	99.2	185	374

Table A.5: Measured densities (kg/m^3) and eigenfrequencies (Hz) for the wood beams of apartment separating wall 3. Beams 1–7 are primary beams and beams 8–9 are edge beams.

Specimen	Density	Eigenfrequencies					
		Bending, width		Bending, height		Torsion	
		First	Second	First	Second	First	Second
1	425	133	–	259	–	559	–
2	483	139	–	274	–	534	–
3	535	144	–	278	–	604	–
4	459	151	–	290	–	539	–
5	355	133	–	258	–	493	–
6	535	146	–	277	–	575	–
7	464	144	–	279	–	534	–
8	510	19.0	52.0	37.7	103	198	400
9	415	18.3	49.6	36.1	99.8	190	388

Table A.6: *Measured densities (kg/m³) and eigenfrequencies (Hz) for the wood beams of apartment separating wall 4. Beams 1–7 are primary beams and beams 8–9 are edge beams.*

| | | Eigenfrequencies | | | | | |
| | | Bending, width | | Bending, height | | Torsion | |
Specimen	Density	First	Second	First	Second	First	Second
1	470	138	–	278	–	563	–
2	416	141	–	270	–	543	–
3	471	140	–	272	–	556	–
4	465	147	–	281	–	560	–
5	459	147	–	286	–	540	–
6	459	148	–	288	–	541	–
7	486	137	–	276	–	579	–
8	489	20.0	53.7	38.5	103	192	389
9	506	20.6	56.2	39.4	–	180	362

Table A.7: *Measured densities (kg/m³) and eigenfrequencies (Hz) for the wood beams of facade wall 1. Beams 1–7 are primary beams and beams 8–9 are edge beams.*

| | | Eigenfrequencies | | | | | |
| | | Bending, width | | Bending, height | | Torsion | |
Specimen	Density	First	Second	First	Second	First	Second
1	411	149	–	449	–	392	–
2	402	122	–	366	–	423	–
3	417	144	–	437	–	–	–
4	391	145	–	435	–	363	–
5	418	146	–	448	–	–	–
6	400	126	–	378	–	–	–
7	387	139	–	415	–	–	–
8	386	19.4	51.5	62.2	164	141	292
9	484	18.8	49.2	59.9	156	139	284

Table A.8: Measured densities (kg/m³) and eigenfrequencies (Hz) for the wood beams of facade wall 2. Beams 1–7 are primary beams and beams 8–9 are edge beams.

Specimen	Density	Eigenfrequencies					
		Bending, width		Bending, height		Torsion	
		First	Second	First	Second	First	Second
1	431	129	–	393	–	421	–
2	407	131	–	421	–	–	–
3	415	150	–	450	–	383	–
4	396	140	–	425	–	–	–
5	417	142	–	393	–	363	–
6	447	153	–	452	–	378	–
7	457	142	–	428	–	422	–
8	416	18.7	51.0	60.0	160	137	286
9	499	21.0	57.3	67.2	179	135	275

Table A.9: Measured densities (kg/m³) and eigenfrequencies (Hz) for the wood beams of facade wall 3. Beams 1–7 are primary beams and beams 8–9 are edge beams.

Specimen	Density	Eigenfrequencies					
		Bending, width		Bending, height		Torsion	
		First	Second	First	Second	First	Second
1	437	152	–	455	–	385	–
2	482	145	–	439	–	–	–
3	483	130	–	389	–	406	–
4	486	146	–	442	–	373	–
5	473	149	–	445	–	–	–
6	445	139	–	426	–	–	–
7	400	126	–	–	–	–	–
8	454	18.2	50.0	57.5	–	140	284
9	401	17.7	48.5	57.9	–	154	–

Table A.10: Measured densities (kg/m^3) and eigenfrequencies (Hz) for the wood beams of facade wall 4. Beams 1–7 are primary beams and beams 8–9 are edge beams.

| Specimen | Density | Eigenfrequencies | | | | | |
| | | Bending, width | | Bending, height | | Torsion | |
		First	Second	First	Second	First	Second
1	455	138	–	412	–	–	–
2	481	154	–	465	–	–	–
3	475	144	–	428	–	356	–
4	471	124	–	381	–	439	–
5	466	141	–	429	–	397	–
6	491	120	–	392	–	405	–
7	417	137	–	424	–	374	–
8	490	18.0	48.6	57.8	153	156	314
9	466	18.9	49.9	61.1	157	155	317

A.1.2 Particleboards and plasterboards

Table A.11: Measured densities (kg/m^3) and eigenfrequencies (Hz) for the particleboards.

| Specimen | Density | Eigenfrequencies | | | | | |
		1	2	3	4	5	6
1	746	36.7	45.6	70.4	85.9	99.7	127
2	748	36.2	44.6	70.0	84.3	98.8	124

Table A.12: Measured densities (kg/m^3) and eigenfrequencies (Hz) for the plasterboards.

| Specimen | Density | Eigenfrequencies | | | | | |
		1	2	3	4	5	6
1	761	23.4	30.4	64.5	67.0	107	114
2	757	23.4	30.4	64.3	66.6	107	114

A.2 PLANAR STRUCTURES

A.2.1 Floor

Table A.13: *Measured eigenfrequencies (Hz) for the floor. *Eigenfrequency lower than the highest frequency of a rigid body mode (4.2 Hz).*

Mode	1	2	3	4	5	6	7	8	9	10
Frequency	3.83*	21.3	32.9	40.4	42.1	49.8	54.0	58.0	62.6	73.1

Mode	11	12	13	14	15	16	17	18
Frequency	74.2	80.0	81.0	83.7	94.6	96.9	97.4	100
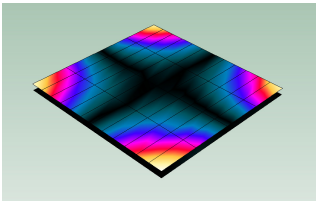
(**a**) 1st mode shape.
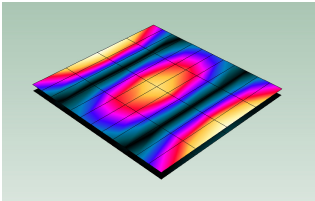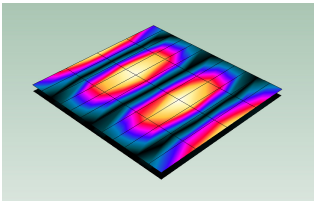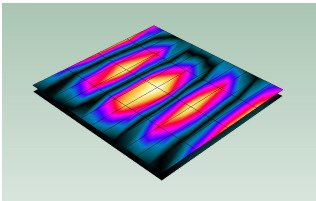
(**b**) 2nd mode shape.

(**c**) 3rd mode shape.
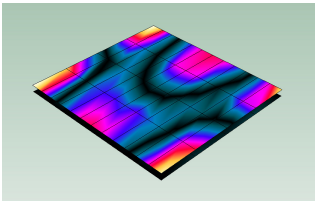
(**d**) 4th mode shape.
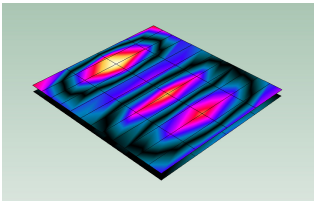
(**e**) 5th mode shape.
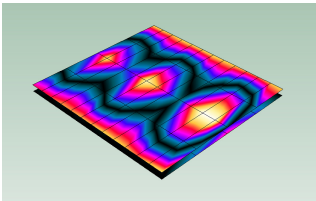
(**f**) 6th mode shape.
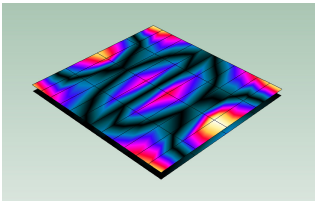
(**g**) 7th mode shape.
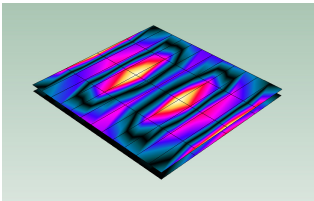
(**h**) 8th mode shape.

(**i**) 9th mode shape.

Figure A.1: *Measured mode shapes (1–9) for the floor.*

(**a**) 10th mode shape.   (**b**) 11th mode shape.   (**c**) 12th mode shape.

(**d**) 13th mode shape.   (**e**) 14th mode shape.   (**f**) 15th mode shape.

(**g**) 16th mode shape.   (**h**) 17th mode shape.   (**i**) 18th mode shape.
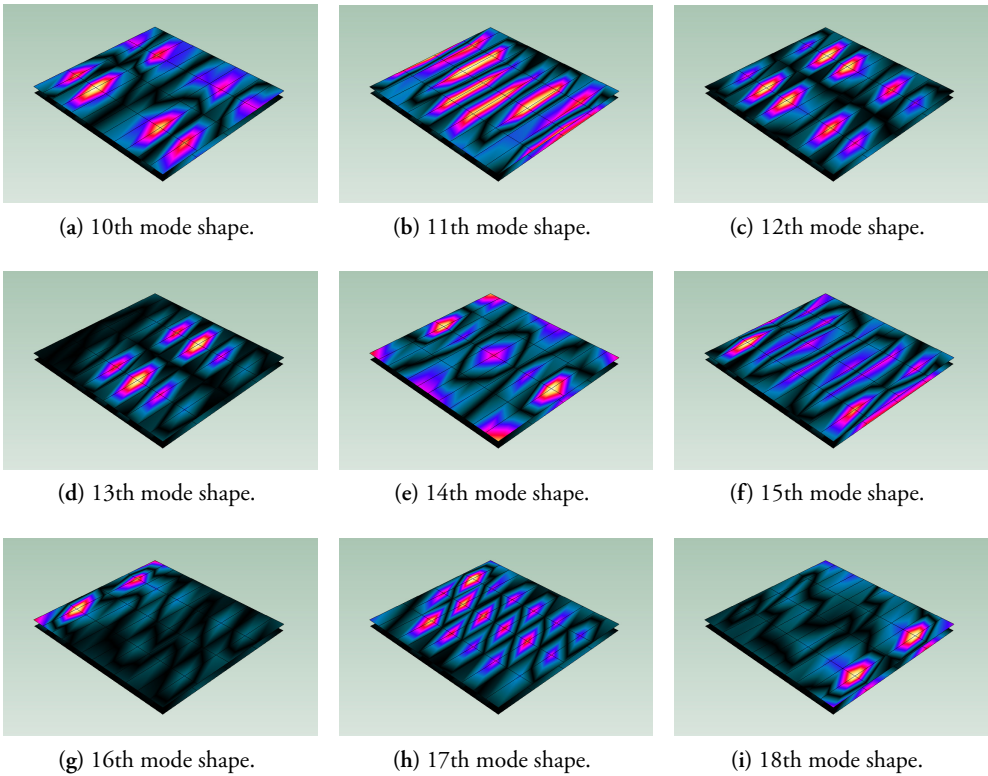
Figure A.2: *Measured mode shapes (10–18) for the floor.*

A.2.2 Ceiling

Table A.14: *Measured eigenfrequencies (Hz) for the ceiling. *Eigenfrequency close to the highest frequency of a rigid body mode (1.4 Hz).*

Mode	1	2	3	4	5	6	7	8	9	10
Frequency	2.87*	11.3	19.5	23.0	24.7	29.1	30.8	34.7	38.0	41.2

Mode	11	12	13	14	15	16	17	18	19	20
Frequency	44.9	47.0	48.6	49.8	56.1	57.8	58.9	59.2	61.7	62.4

Mode	21	22	23	24	25	26	27	28	29	30
Frequency	64.0	68.3	73.1	74.2	75.9	77.1	78.6	80.3	81.3	83.9

Mode	31	32	33	34	35	36	37
Frequency	86.9	88.4	90.9	92.3	97.8	99.2	99.7
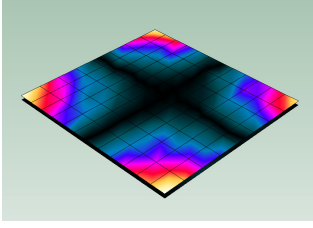
(**a**) 1st mode shape.
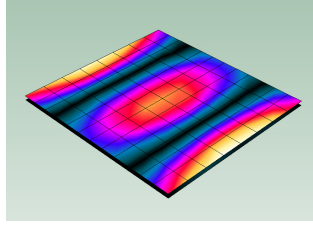
(**b**) 2nd mode shape.
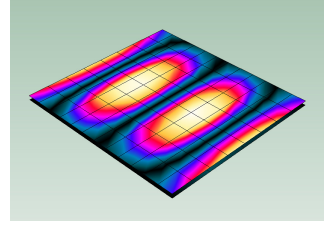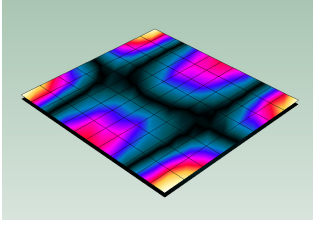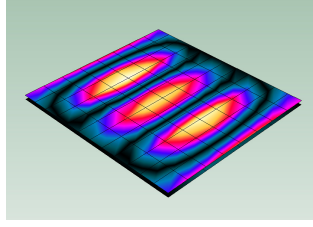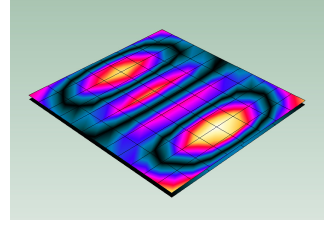
(**c**) 3rd mode shape.

(**d**) 4th mode shape.

(**e**) 5th mode shape.
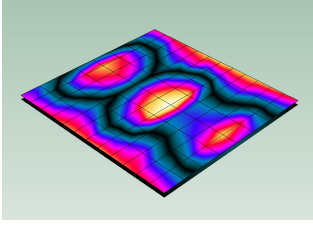
(**f**) 6th mode shape.
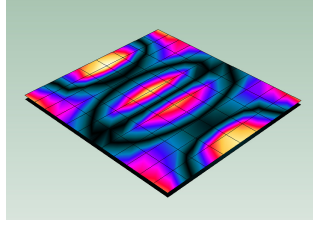
(**g**) 7th mode shape.
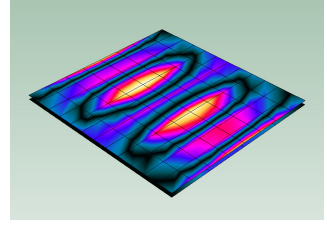
(**h**) 8th mode shape.
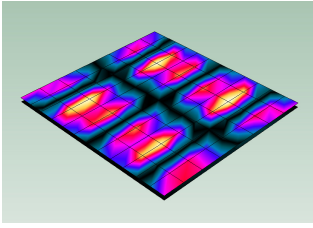
(**i**) 9th mode shape.
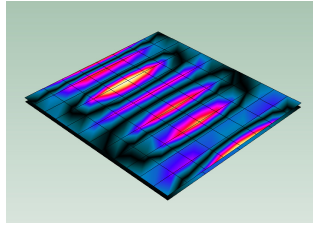
(**j**) 10th mode shape.
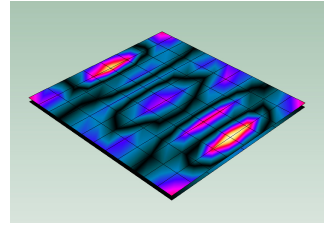
(**k**) 11th mode shape.

(**l**) 12th eigenmode.
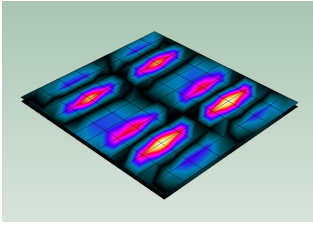
(**m**) 13th mode shape.
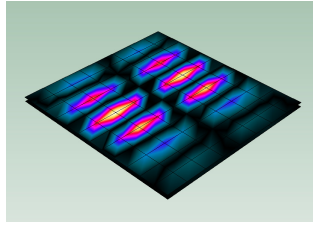
(**n**) 14th mode shape.
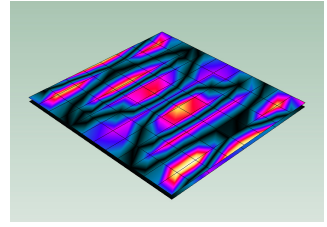
(**o**) 15th mode shape.

Figure A.3: Measured mode shapes (1–15) for the ceiling.
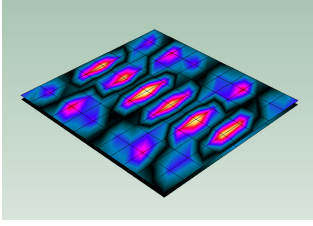
(a) 16th mode shape.
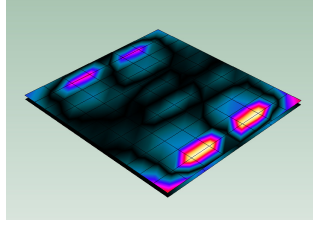
(b) 17th mode shape.
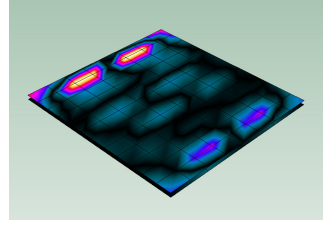
(c) 18th mode shape.
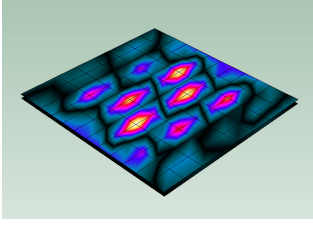
(d) 19th mode shape.
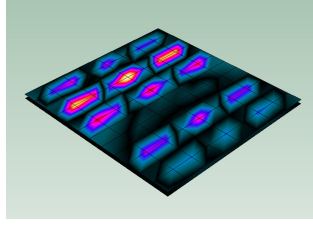
(e) 20th mode shape.
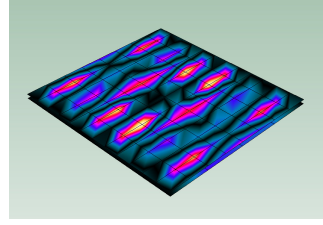
(f) 21th mode shape.
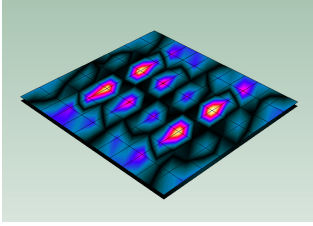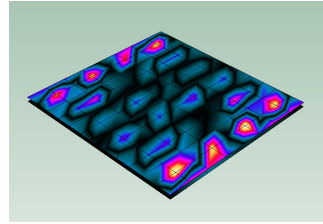
(g) 22th mode shape.
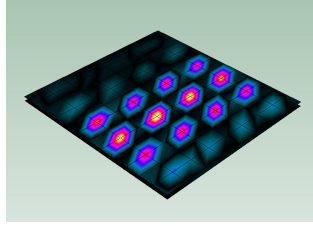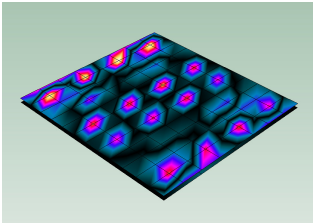
(h) 23th mode shape.
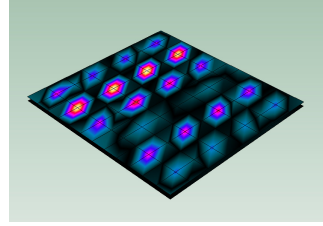
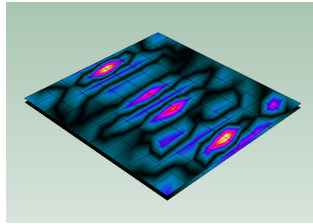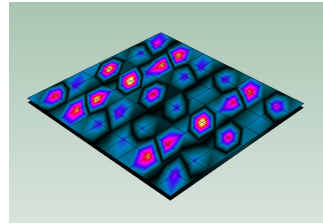(i) 24th mode shape.
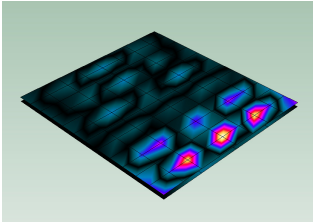
(j) 25th mode shape.
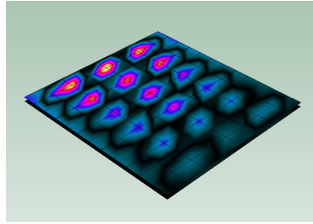
(k) 26th mode shape.
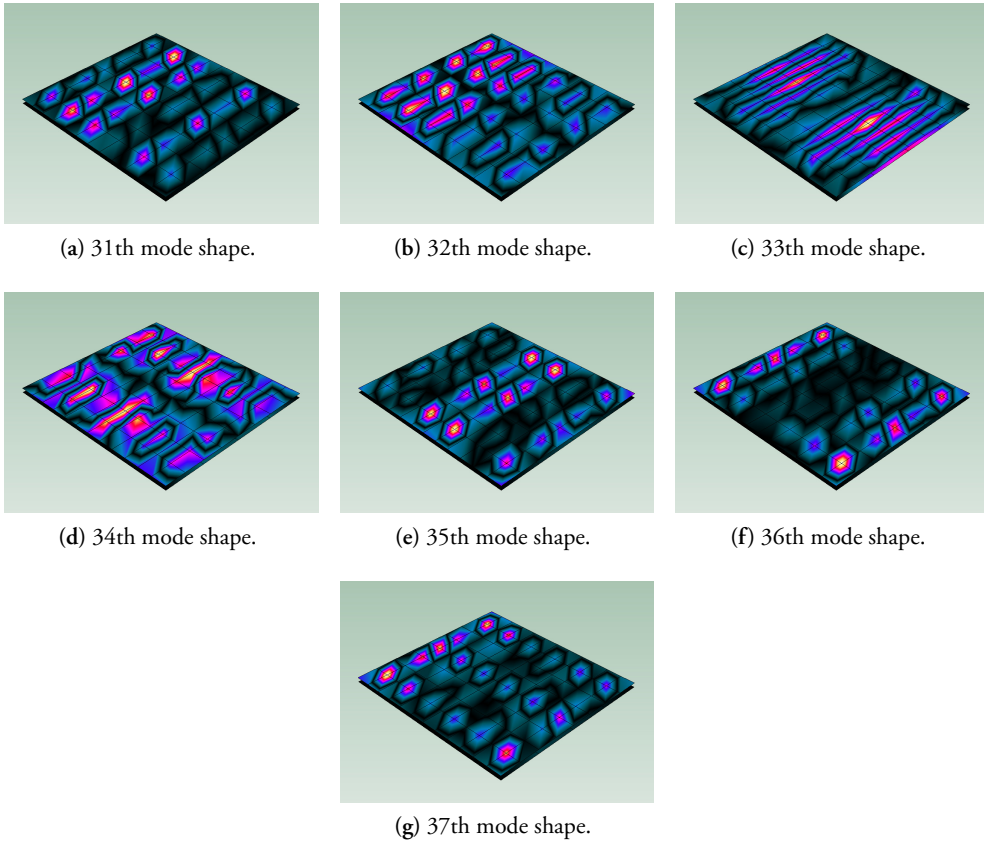
(l) 27th mode shape.

(m) 28th mode shape.

(n) 29th mode shape.

(o) 30th mode shape.

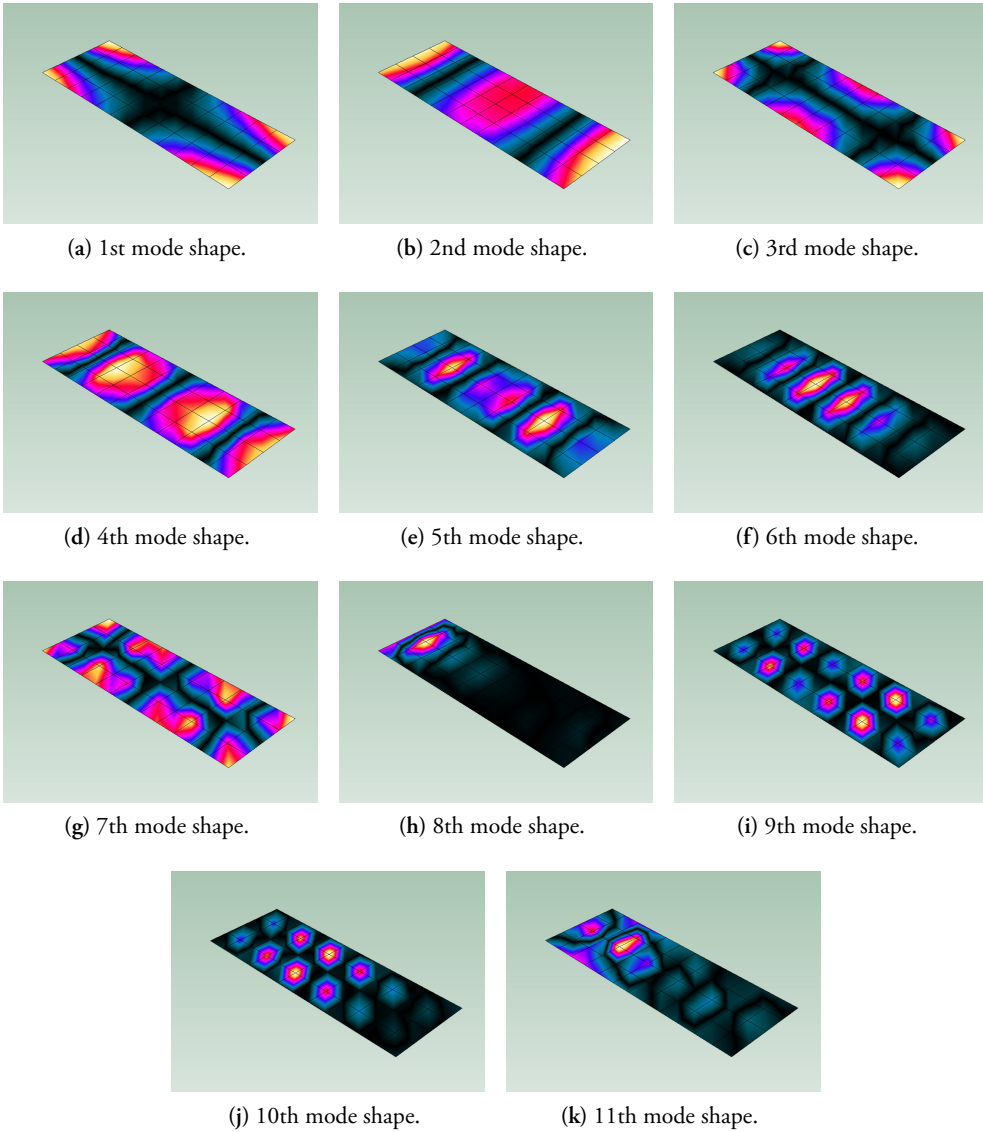*Figure A.4: Measured mode shapes (16–30) for the ceiling.*

(**a**) 31th mode shape.

(**b**) 32th mode shape.

(**c**) 33th mode shape.

(**d**) 34th mode shape.

(**e**) 35th mode shape.

(**f**) 36th mode shape.

(**g**) 37th mode shape.

Figure A.5: *Measured mode shapes (31–37) for the ceiling.*

A.2.3 Apartment separating walls

Table A.15: *Measured eigenfrequencies (Hz) for the apartment separating walls.*

Wall	Eigenfrequencies											
	1	2	3	4	5	6	7	8	9	10	11	12
1	6.84	19.5	29.6	40.2	52.8	56.9	67.8	75.0	75.4	86.7	95.3	97.2
2	6.34	19.8	29.2	40.9	54.2	59.7	68.6	80.1	88.3	90.3	94.5	98.6
3	6.29	19.8	29.2	40.6	54.6	60.9	67.7	78.8	88.3	92.2	96.6	–
4	6.33	20.2	29.0	42.0	55.6	60.9	69.9	76.6	90.2	91.7	95.2	–

(**a**) 1st mode shape.

(**b**) 2nd mode shape.

(**c**) 3rd mode shape.

(**d**) 4th mode shape.

(**e**) 5th mode shape.

(**f**) 6th mode shape.

(**g**) 7th mode shape.

(**h**) 8th mode shape.

(**i**) 9th mode shape.

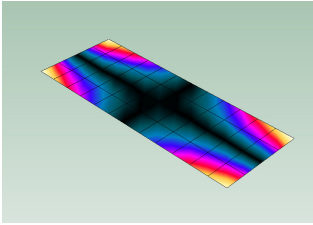(**j**) 10th mode shape.

(**k**) 11th mode shape.

Figure A.6: *Measured mode shapes for apartment separating wall 4.*

A.2.4 Facade walls

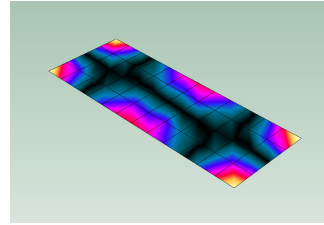*Table A.16: Measured eigenfrequencies (Hz) for the facade walls.*

Wall	Eigenfrequencies									
	1	2	3	4	5	6	7	8	9	10
1	7.30	32.7	46.3	59.4	66.8	90.9	92.4	96.3	98.1	–
2	7.20	32.9	47.9	59.3	64.6	66.3	89.5	89.8	91.6	96.6
3	7.58	30.6	43.5	58.6	66.9	67.6	87.7	90.4	92.2	98.4
4	7.88	31.7	45.3	58.4	66.1	89.3	88.5	95.8	–	–

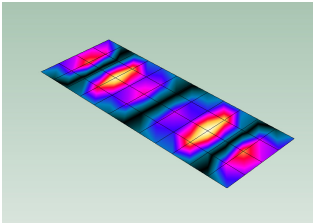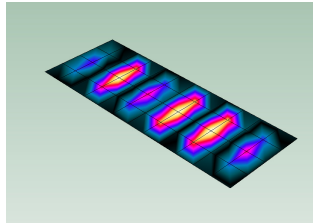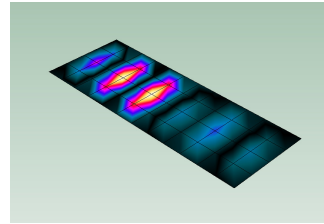(**a**) 1st mode shape.
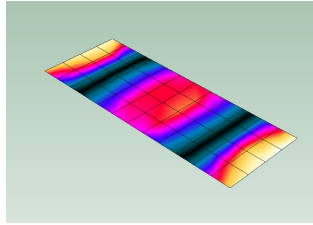
(**b**) 2nd mode shape.
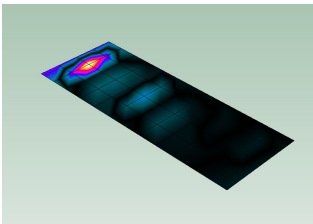
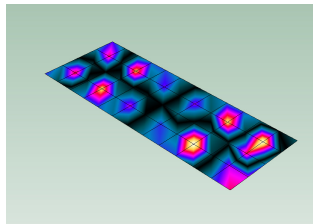(**c**) 3rd mode shape.

(**d**) 4th mode shape.
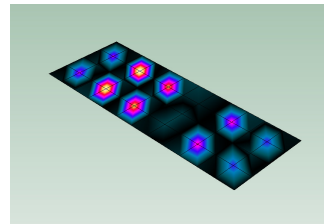
(**e**) 5th mode shape.

(**f**) 6th mode shape.

(**g**) 7th mode shape.

(**h**) 8th mode shape.

(**i**) 9th mode shape.

Figure A.7: Measured mode shapes for facade wall 3.

A.3 ROOMS

A.3.1 Upper room

Table A.17: Measured eigenfrequencies (Hz) and damping ratios (%) for the upper room.

Mode	1	2	3	4	5	6	7	8	9
Frequency	15.9	18.0	19.9	22.0	30.0	32.7	34.2	38.4	39.3
Damping	1.61	1.48	1.02	0.908	1.57	1.80	0.899	1.16	1.06

Mode	10	11
Frequency	40.2	49.3
Damping	0.876	1.00

(**a**) 1st mode shape. (**b**) 2nd mode shape. (**c**) 3rd mode shape.
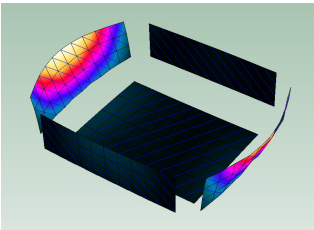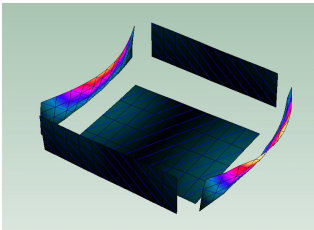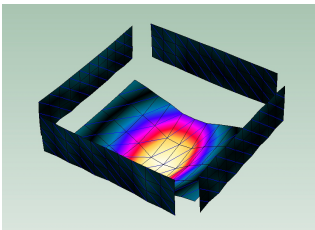
(**d**) 4th mode shape. (**e**) 5th mode shape. (**f**) 6th mode shape.
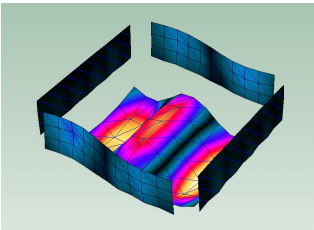
(**g**) 7th mode shape. (**h**) 8th mode shape. (**i**) 9th mode shape.
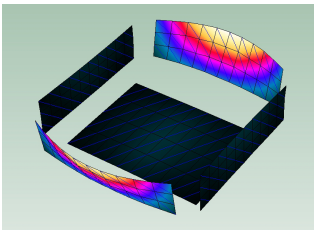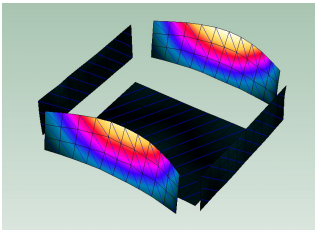
Figure A.8: Measured mode shapes (1–9) for the upper room.

(a) 10th mode shape.

(b) 11th mode shape.
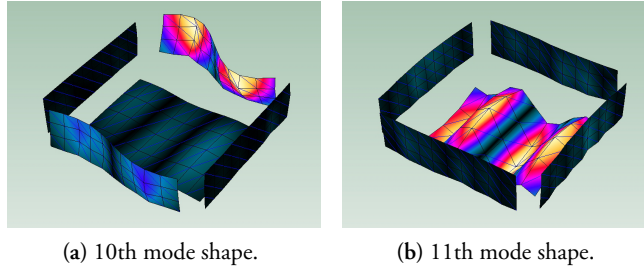
Figure A.9: Measured mode shapes (10–11) for the upper room.

A.3.2 Lower room

Table A.18: Measured eigenfrequencies (Hz) and damping ratios (%) for the lower room.

Mode	1	2	3	4	5	6	7	8	9
Frequency	13.8	16.9	18.5	19.3	20.3	21.9	24.6	30.3	36.9
Damping	1.62	1.70	1.21	1.48	1.22	1.21	1.18	1.06	1.20

| Mode	10	11	12	13	14
Frequency	37.6	39.1	44.2	47.2	47.7
Damping	0.996	1.08	1.11	1.06	1.17

(a) 1st mode shape.

(b) 2nd mode shape.
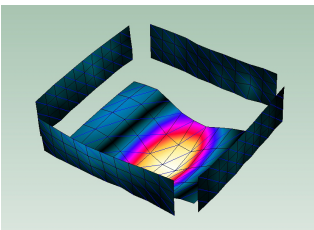
(c) 3rd mode shape.

(d) 4th mode shape.

(e) 5th mode shape.
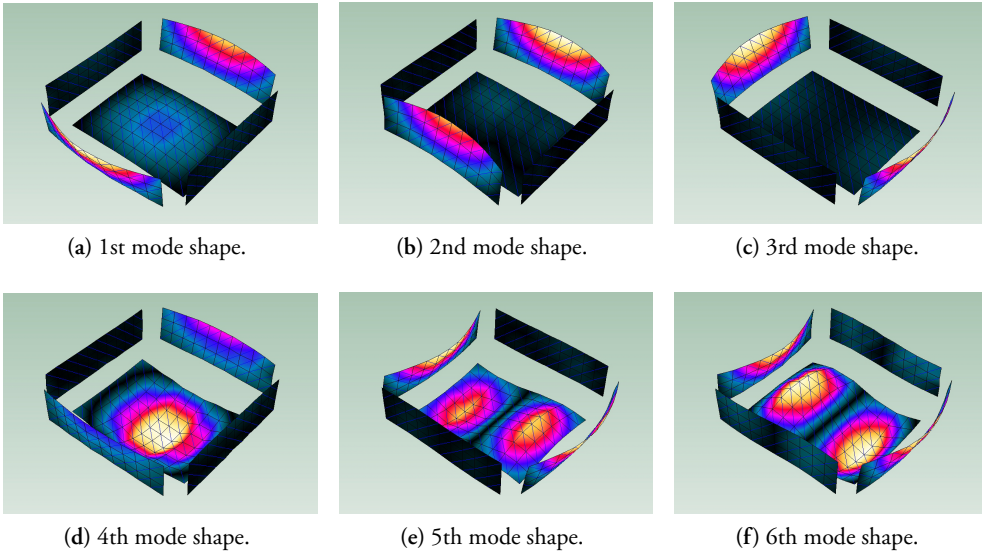
(f) 6th mode shape.

Figure A.10: Measured mode shapes (1–6) for the lower room.

(a) 7th mode shape.

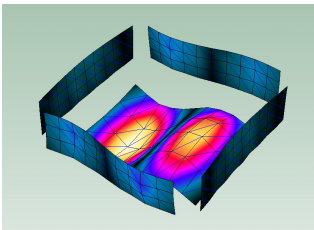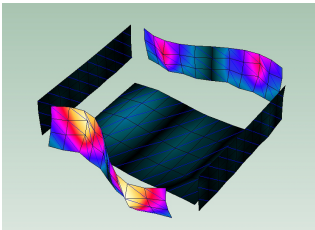(b) 8th mode shape.

(c) 9th mode shape.

(d) 10th mode shape.

(e) 11th mode shape.


(f) 12th mode shape.

(g) 13th mode shape.

(h) 14th mode shape.
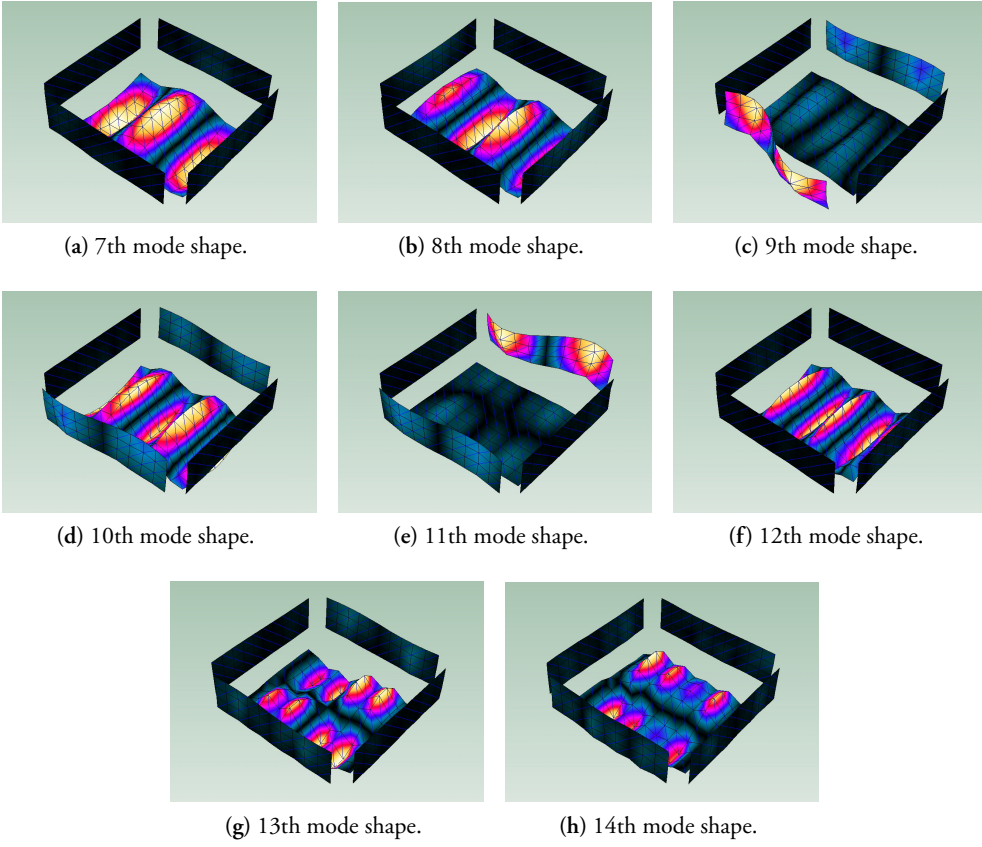
Figure A.11: *Measured mode shapes (7–14) for the lower room.*

A.4 COMPLETE STRUCTURE
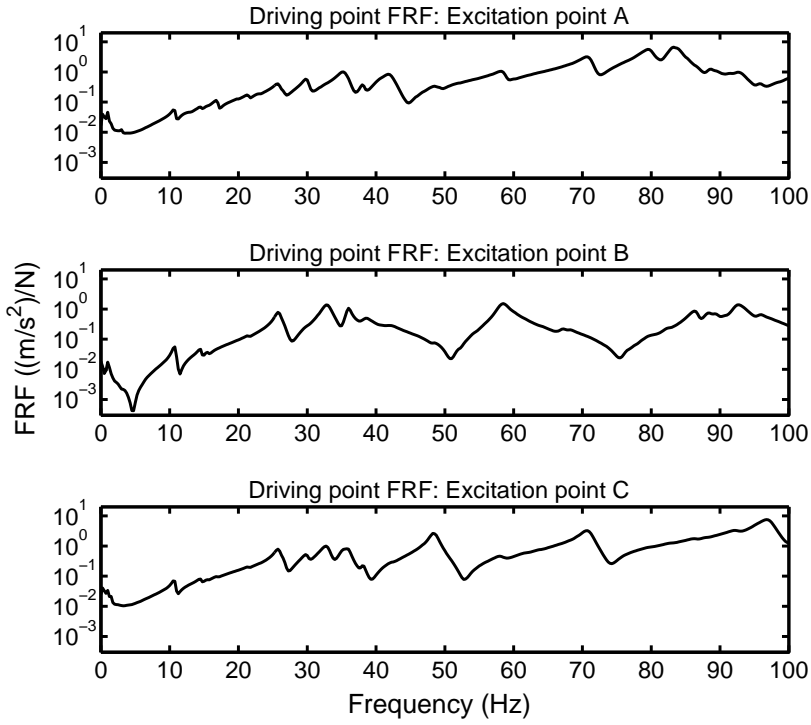
Figure A.12: Driving point FRFs for the excitation points on the floor.
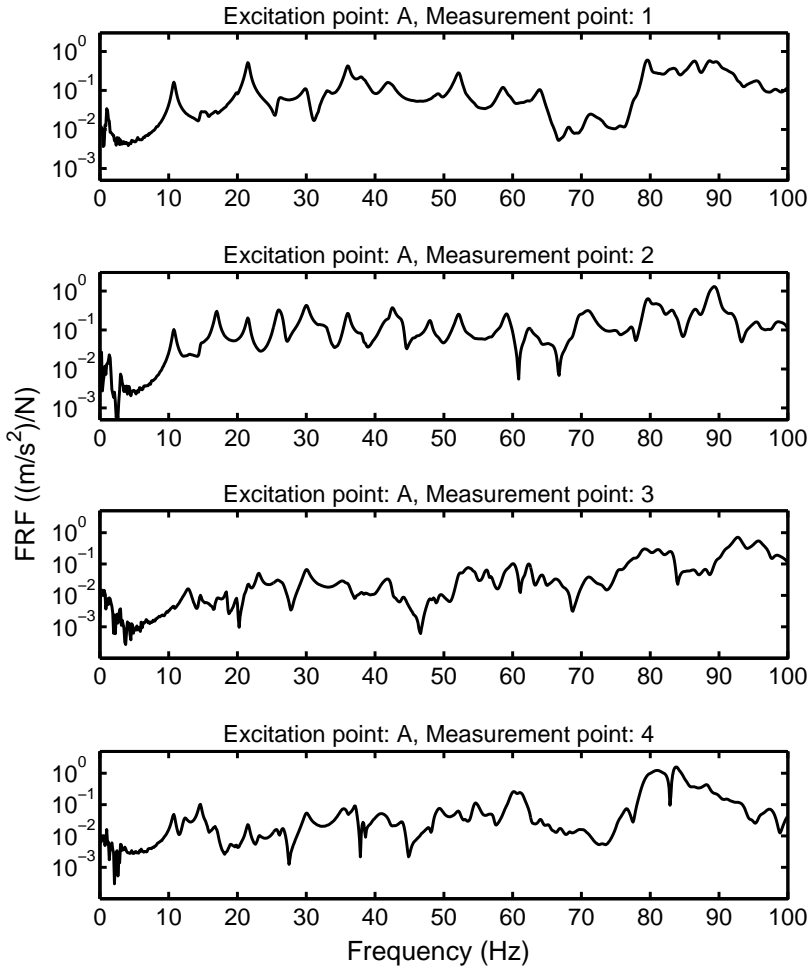
Figure A.13: *FRFs for the transmission from excitation point A on the floor in the upper room to the measurement points on the ceiling and walls in the lower room.*
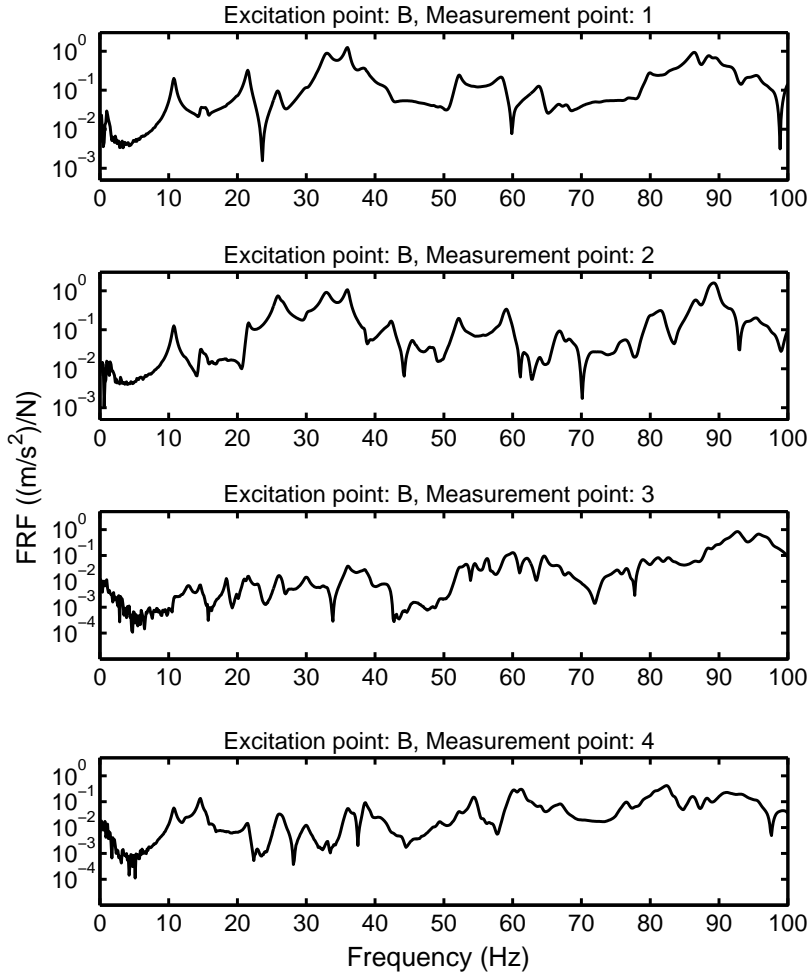
Figure A.14: *FRFs for the transmission from excitation point B on the floor in the upper room to the measurement points on the ceiling and walls in the lower room.*
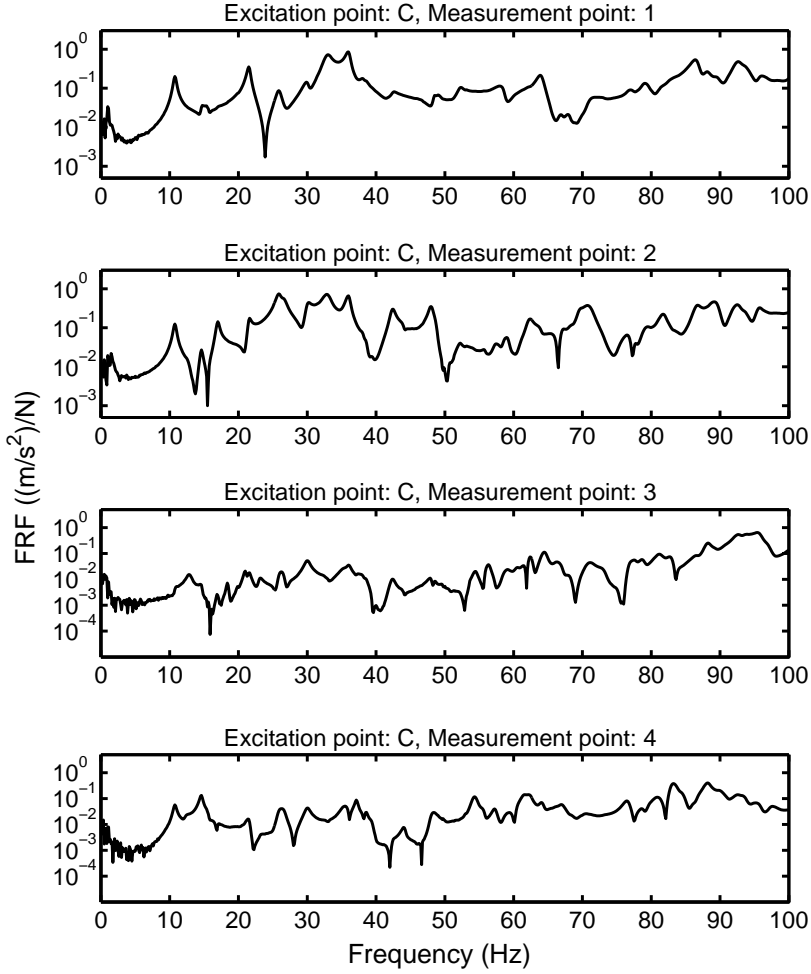
Figure A.15: *FRFs for the transmission from excitation point C on the floor in the upper room to the measurement points on the ceiling and walls in the lower room.*

B Optimised material parameters

B.1 WOOD BEAMS

Table B.1: *Optimised material parameters (in the unit of GPa) for the wood beams in the floor. Beams 1–7 are primary beams and beams 8–9 are edge beams.*

Beam	1	2	3	4	5	6	7	8	9
E_L	11.8	14.4	15.0	10.1	14.9	11.3	11.5	10.9	12.2
$G_{LR} = G_{LT}$	0.747	0.817	0.761	0.532	0.751	0.672	0.645	0.719	0.805

Table B.2: *Optimised material parameters (in the unit of GPa) for the wood beams in the ceiling. Beams 1–7 are primary beams and beams 8–9 are edge beams.*

| Beam	1	2	3	4	5	6	7	8	9
E_L	12.4	11.0	13.9	14.4	12.2	11.3	16.7	13.7	10.6
$G_{LR} = G_{LT}$	0.633	0.726	0.632	0.780	0.640	0.775	0.695	0.989	0.638

Table B.3: *Optimised material parameters (in the unit of GPa) for the wood beams in apartment separating wall 1. Beams 1–7 are primary beams and beams 8–9 are edge beams.*

Beam	1	2	3	4	5	6	7	8	9
E_L	10.5	7.16	11.5	11.0	9.69	11.6	10.7	12.1	11.5
$G_{LR} = G_{LT}$	0.834	0.712	0.925	0.881	0.686	0.874	0.911	0.789	0.607

Table B.4: *Optimised material parameters (in the unit of GPa) for the wood beams in apartment separating wall 2. Beams 1–7 are primary beams and beams 8–9 are edge beams.*

Beam	1	2	3	4	5	6	7	8	9
E_L	6.57	13.0	11.0	7.77	8.70	9.91	9.04	10.9	12.7
$G_{LR} = G_{LT}$	0.583	1.04	0.806	0.547	0.696	0.872	0.745	0.806	0.756

Table B.5: *Optimised material parameters (in the unit of GPa) for the wood beams in apartment separating wall 3. Beams 1–7 are primary beams and beams 8–9 are edge beams.*

Beam	1	2	3	4	5	6	7	8	9
E_L	8.82	11.1	12.7	12.2	7.54	12.5	10.9	13.3	9.99
$G_{LR} = G_{LT}$	0.799	0.814	1.16	0.786	0.590	1.03	0.775	0.894	0.680

Table B.6: *Optimised material parameters (in the unit of GPa) for the wood beams in apartment separating wall 4. Beams 1–7 are primary beams and beams 8–9 are edge beams.*

Beam	1	2	3	4	5	6	7	8	9
E_L	10.5	9.26	10.4	11.2	11.3	11.5	10.7	13.4	15.1
$G_{LR} = G_{LT}$	0.879	0.728	0.856	0.858	0.785	0.787	0.961	0.811	0.731

Table B.7: *Optimised material parameters (in the unit of GPa) for the wood beams in facade wall 1. Beams 1–7 are primary beams and beams 8–9 are edge beams.*

Beam	1	2	3	4	5	6	7	8	9
E_L	11.3	7.37	10.7	10.1	11.0	7.91	9.26	10.4	12.0
$G_{LR} = G_{LT}$	0.664	0.642	0.678	0.616	0.680	0.638	0.607	0.679	0.817

Table B.8: *Optimised material parameters (in the unit of GPa) for the wood beams in facade wall 2. Beams 1–7 are primary beams and beams 8–9 are edge beams.*

Beam	1	2	3	4	5	6	7	8	9
E_L	8.80	8.63	11.6	9.60	10.4	12.9	11.3	11.0	9.43
$G_{LR} = G_{LT}$	0.725	0.831	0.834	0.841	0.810	0.744	0.638	0.698	0.790

Table B.9: *Optimised material parameters (in the unit of GPa) for the wood beams in facade wall 3. Beams 1–7 are primary beams and beams 8–9 are edge beams.*
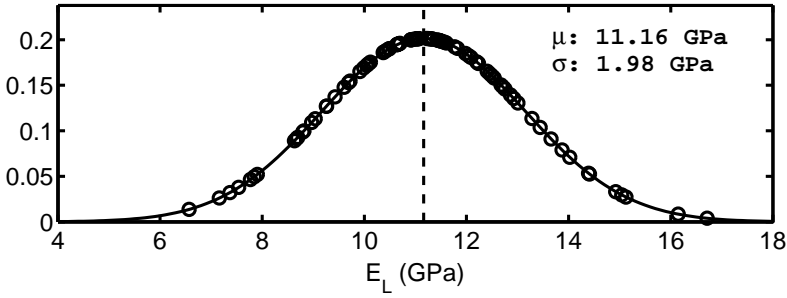
Beam	1	2	3	4	5	6	7	8	9
E_L	12.5	12.5	10.0	12.8	12.9	10.7	7.84	10.6	16.1
$G_{LR} = G_{LT}$	0.711	0.654	0.673	0.628	0.678	0.749	0.772	0.773	0.464

Table B.10: *Optimised material parameters (in the unit of GPa) for the wood beams in facade wall 4. Beams 1–7 are primary beams and beams 8–9 are edge beams.*
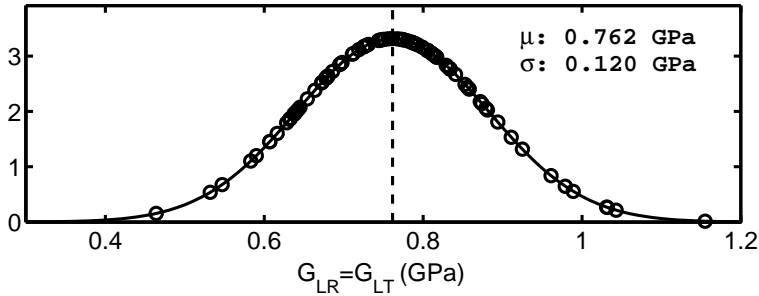
Beam	1	2	3	4	5	6	7	8	9
E_L	10.7	14.0	12.0	8.97	11.5	8.67	9.72	11.4	11.8
$G_{LR} = G_{LT}$	0.768	0.829	0.815	0.805	0.794	0.853	0.678	1.03	0.979

Figure B.1: *Normal distribution for the optimised values of the elastic modulus E_L, based on the results for all 90 wood beams. The circles represent optimised values. μ is the mean value and σ is the standard deviation.*

Figure B.2: *Normal distribution for the optimised values of the shear modulus $G_{LR} = G_{LT}$, based on the results for all 90 wood beams. The circles represent optimised values. μ is the mean value and σ is the standard deviation.*

B.2 PARTICLEBOARDS AND PLASTERBOARDS

Table B.11: Optimised material parameters (in the unit of GPa) for the particleboard specimens.

Specimen	1	2
E_1	4.66	4.44
E_2	4.39	4.36
G_{12}	1.92	1.88

Table B.12: Optimised material parameters (in the unit of GPa) for the plasterboard specimens.

Specimen	1	2
E_1	3.97	3.97
E_2	3.09	3.06
G_{12}	1.35	1.33